Excited states in ^{155}Yb and ^{155,156,157}Lu from recoil-decay tagging

K. Y. Ding,[1,*] J. A. Cizewski,[1] D. Seweryniak,[2] H. Amro,[2,†] M. P. Carpenter,[2] C. N. Davids,[2] N. Fotiades,[1,‡] R. V. F. Janssens,[2] T. Lauritsen,[2] C. J. Lister,[2] D. Nisius,[2,§] P. Reiter,[2,‖] J. Uusitalo,[2,¶] I. Wiedenhöver,[2] and A. O. Macchiavelli[3]

[1]*Department of Physics and Astronomy, Rutgers University, New Brunswick, New Jersey 08903*

[2]*Argonne National Laboratory, Argonne, Illinois 60439*

[3]*Nuclear Science Division, Lawrence Berkeley National Laboratory, Berkeley, California 94720*

(Received 2 April 2001; published 22 August 2001)

The 270-MeV ^{58}Ni+ ^{102}Pd reaction was used for the first recoil-decay tagging measurement with Gammasphere coupled to the Fragment Mass Analyzer at Argonne National Laboratory. Level structures of ^{155}Yb, ^{156}Lu, and ^{157}Lu, as well as the excited states associated with the $25/2^-$ isomer in ^{155}Lu, are identified for the first time. The systematical behavior of the energy levels is compared with that of neighboring isotones and isotopes. The attractive interaction between $h_{11/2}$ protons and $h_{9/2}$ neutrons plays an important role in the structure of ^{155}Yb and ^{155,156}Lu.

DOI: 10.1103/PhysRevC.64.034315 PACS number(s): 23.20.Lv, 23.20.En, 27.70.+q

I. INTRODUCTION

The region of proton-rich $N=84$ isotones above ^{146}Gd has received considerable attention, e.g., Ref. [1], since the identification of ^{146}Gd as a doubly magic nucleus [2,3]. The orbitals in the $50<Z\leqslant 82$ major shell are $1g_{7/2}$, $2d_{5/2}$, $3s_{1/2}$, $1h_{11/2}$, and $2d_{3/2}$. ^{146}Gd has a filled $N=82$ neutron shell and the protons fill the $1g_{7/2}$ and $2d_{5/2}$ orbitals. Evidence such as a high excitation energy for the 2^+ state [3], the presence of a collective, low-lying 3^- state similar to that observed in doubly magic ^{208}Pb [2], and the direct measurement of the $Z=64$ gap size from proton separation energies [4], indicated that ^{146}Gd can be regarded as a doubly magic nucleus with a large energy gap between the proton $1g_{7/2}$ and $2d_{5/2}$ orbitals and the remaining $1h_{11/2}$, $3s_{1/2}$, and $2d_{3/2}$ orbitals.

The $N=84$ isotones with $Z\geqslant 64$ are spherical nuclei. High-spin states involve protons occupying the $h_{11/2}$ orbital and neutrons in the $f_{7/2}$, $h_{9/2}$, and $i_{13/2}$ orbitals. The configurations of the excited states are mainly of the type $\pi h_{11/2}^n \nu f_{7/2}^m$ and $\pi h_{11/2}^n \nu f_{7/2}^m h_{9/2}^r$. At high excitation energies, $i_{13/2}$ neutrons also play a significant role in high-spin states. The excited states are generated by the gradual alignment of the spin of the individual nucleons. The study of excitations in the proton-rich $N=84$ isotones can probe the interactions between the two neutrons in the $f_{7/2}$ and $h_{9/2}$ orbitals above the $N=82$ gap, and also the interactions between these neutrons and protons in the $h_{11/2}$ orbital above the $Z=64$ gap. The primary purpose of the present measurement was to study the excited states in the proton-rich $N=84$ isotones above the ^{146}Gd core.

Shell model calculations predicted that the strong attractive interaction between protons in the $h_{11/2}$ orbital and neutrons in the $h_{9/2}$ orbital could result in a change in the shell structure [5]. This effect is manifested through lower excitation energies for the $h_{9/2}$ neutron excitations with respect to $f_{7/2}$ states, and can result in the formation of isomers, which have been observed in the $N=83$ and 84 isotones, e.g., Refs. [6,7]. Excitations built on high-spin isomers in the $N=84$ ^{155}Lu and ^{156}Hf [8] nuclei have been previously identified in γ-ray spectroscopy. The present study of the excited states built upon the high-spin isomers in ^{155}Lu and ^{156}Lu investigates the strength of the attractive interaction between $h_{9/2}$ neutrons and $h_{11/2}$ protons as a function of proton number. Since the $N=84$ isotones with $Z\geqslant 64$ approach the proton-drip line, the present work will also investigate possible changes in the proton-neutron interaction for systems in which the last proton is only weakly bound.

II. EXPERIMENT

The ^{102}Pd(^{56}Ni,$xpyn$) reaction at $E_{\text{beam}}=270$ MeV was used to populate the high-spin states in the proton-rich nuclei above the ^{146}Gd core. The projectile, ^{58}Ni, was accelerated by the Argonne Tandem Linear Accelerator System (ATLAS) on a 1-mg/cm^2 ^{102}Pd target with 69% enrichment. The major target contaminants were ^{104}Pd (12%), ^{105}Pd (6%), and ^{106}Pd (6%). The proton-rich ^{160}W compound system has a large number of exit channels and fusion evaporation has strong competition from the dominant fission process. The exit channels to be discussed in this work are ^{155}Yb ($4pn$), ^{155}Lu ($3p2n$), ^{156}Lu ($3pn$), and ^{157}Lu ($3p$). The level schemes of ^{158,159,160}Hf, produced in reactions with the heavier Pd isotopes in the target, are presented elsewhere [9].

Gammasphere (GS), with 101 Ge detectors, coupled to the Fragment Mass Analyzer (FMA) [10], was used for γ-ray spectroscopy. The compound nuclei which recoil from the target were dispersed according to their mass-to-charge

*Present address: Telcordia Technologies, Piscataway, NJ 08854.

†Present address: Mississippi State University, Mississippi St., MS 39762.

‡Present address: Los Alamos National Laboratory, Los Alamos, NM 87545.

§Present address: Bio-Imaging Research, Lincolnshire, IL 60069.

‖Present address: Ludwig Maximilian Universität München, Garching, Germany.

¶Present address: University of Jyväskylä, 40351 Jyväskylä, Finland.

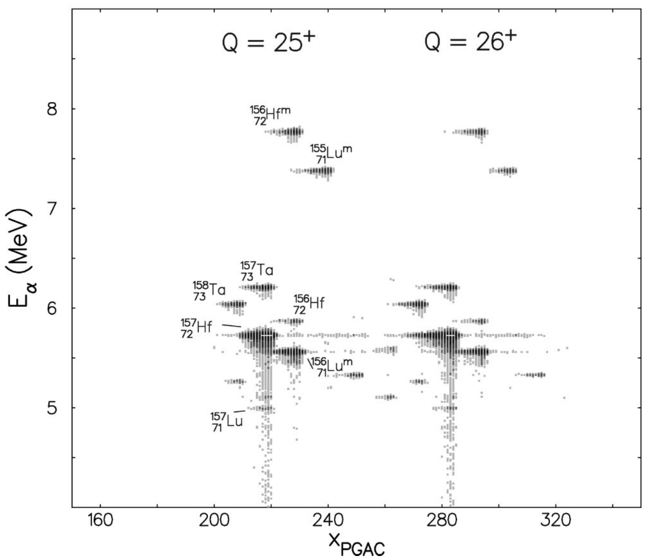

FIG. 1. Two-dimensional display of the E_α vs X_{PGAC} matrix for decays which occurred within 200 ms after implantation.

(M/Q) ratio by the FMA. The positions of the recoils at the focal plane of the FMA were determined using a position-sensitive parallel-grid avalanche counter (PGAC). The recoils were implanted in a 48×48 double-sided silicon-strip detector (DSSD) placed 40 cm behind the PGAC.

The data from the experiment were recorded using the GS data acquisition system and written to magnetic tapes for off-line analysis. The pretrigger condition required at least two Compton-suppressed Ge detectors to fire. The main trigger of an event required signals from at least two Ge detectors and the PGAC, or any event in which the DSSD recorded a recoil or decay event. The time delay between the pre- and main triggers was 850 ns to allow sufficient time for the recoils to traverse the FMA and determine if a PGAC event occurred at the focal plane. The correlations between implant and decay events from the DSSD were established in the off-line analysis.

Standard γ-ray sources of ^{152}Eu, ^{182}Ta, ^{56}Co, and ^{243}Am were used for energy and efficiency calibrations of the Ge detectors. Angular distributions of the γ-ray intensities were mainly used to deduce the multipolarity of a transition when directional correlation (DCO) analyses were not available because of insufficient statistics.

The FMA was set up to allow both the 25^+ and 26^+ charge states of $A=155,156,157$ recoils to be collected at the focal plane. The projection of the X_{PGAC} vs E_γ matrix onto the X_{PGAC} axis was shown in Fig. 1 of Ref. [9]. The strongest channel, with mass $M=157$, is ^{157}Lu, the $3p$ evaporation channel.

The recoil-decay tagging (RDT) technique [11] was used to select specific isomers that have the same X_{PGAC} position. A matrix of E_α vs X_{PGAC} with the condition that the decay occurred within 200 ms of the implant is displayed in Fig. 1. The data illustrate clearly that the correlations are unambiguous and that assignments are easy to make on this basis. The correlations between the prompt γ rays, mass of the implant, and decay of the implant were established off line. Additional details of the experimental procedures and γ-ray analyses are given in Refs. [9,12].

III. ANALYSIS AND RESULTS

A. Level scheme of ^{155}Lu

Three α decaying isomers have been identified in ^{155}Lu: the ground state with $E_\alpha=5.584$ MeV and half-life $t_{1/2}=136$ ms and high-spin isomers with spins $11/2^-$ and $25/2^-$, $E_\alpha=5.655$ and 7.390 MeV, and $t_{1/2}=70$ and 2.71 ms, respectively [13].

The ground-state spin-parity was suggested to be $3/2^+$ with the unpaired proton occupying the $d_{3/2}$ orbital [14]. The excitations above the $3/2^+$ state are weakly populated in the present heavy-ion fusion reaction, because these levels are above the yrast line. No transitions above the $3/2^+$ state have been placed.

Prior to this work, transitions at 537, 686, and 807 keV had been identified and correlated with the α decays from the $11/2^-$ isomer [8]. These transitions were assigned to the states above the $11/2^-$ isomer and arise from coupling the unpaired $h_{11/2}$ proton to the $(\nu f_{7/2})^2_{0^+,2^+,4^+,6^+}$ states in the neutron core. In the present data, the transitions at 686 and 807 keV were observed, but not the one at 537 keV. Due to insufficient γ-γ statistics, the ordering of these transitions above the $11/2^-$ isomer cannot be confirmed by the present measurement. The low statistics of this cascade is attributed to the pretrigger condition of GS, which required at least two Ge detectors to fire. With a cascade of only three transitions and taking the GS efficiency into account, the probability to detect two coincident γ rays is one-tenth that of detecting one γ ray. Spectra gated on the $3/2^+$ and $11/2^-$ isomers in ^{155}Lu are presented in Ref. [12].

The total projection of the recoil- and α-gated γ-ray events associated with the $25/2^-$ isomer in ^{155}Lu is shown in Fig. 2(a). The assignment of these transitions to Lu isotopes is confirmed by the presence of the Lu x rays in this spectrum.

The excited states above the $25/2^-$ isomer in ^{155}Lu are studied for the first time. A γ-γ coincidence matrix was constructed by gating on mass $A=155$ and the 7.390-MeV α line from the decay of the $25/2^-$ isomer. A coincidence spectrum gated on the 518.8-keV transition in this matrix is shown in Fig. 2(b). This transition is in coincidence with all of the other transitions in Fig. 2(a) that feed the $25/2^-$ isomer. The level structure above the $25/2^-$ isomer, as well as that above the $11/2^-$ isomer taken from Ref. [8], are presented in Fig. 3. The transitions are arranged according to their intensities and coincidence relationships. The γ-ray results are summarized in Table I; the relative intensities of the transitions are from the total projection gated on both mass $=155$ and the α decay from the $25/2^-$ isomer. The intensities of the γ rays observed in ^{155}Lu are too weak to determine their multipolarity. The tentative assignments of the $25/2^-$, $27/2^-$, $29/2^+$, and $31/2^+$ states are based on the systematics of the $N=84$ isotones [1,15].

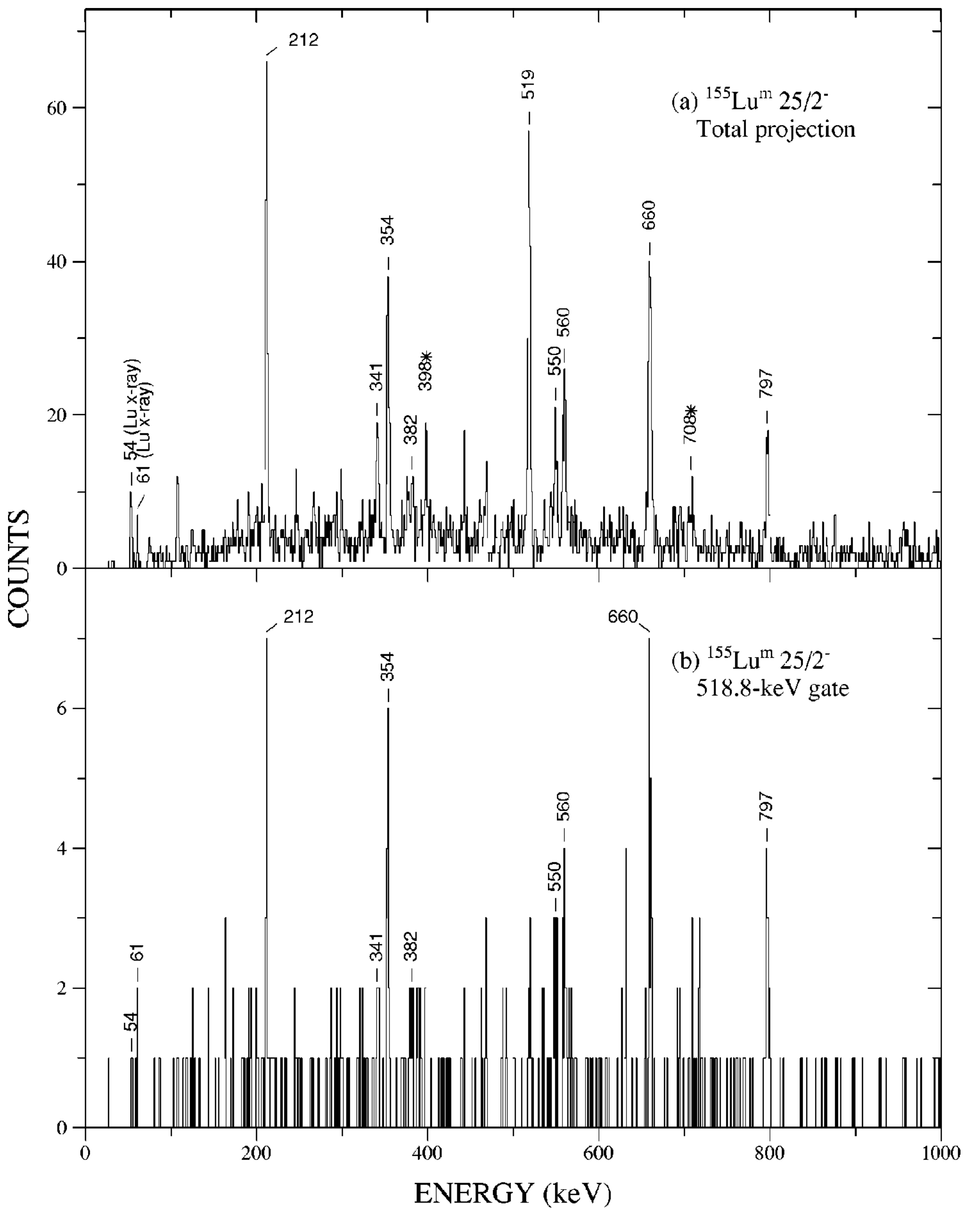

FIG. 2. (a) Total projection of the γ-ray events gated on mass $=155$ and the α decays from the $25/2^{-}$ isomer in ^{155}Lu with $E_\alpha=7.390$ MeV and $t_{1/2}=2.7$ ms. The transitions marked with an asterisk have not been placed in the level scheme. (b) Background-subtracted coincidence spectrum gated on the 518.8-keV transition that feeds the $25/2^{-}$ isomer in ^{155}Lu.

B. Level scheme of ^{155}Yb

The high-spin isomer in ^{155}Yb decays with $E_\alpha=5.202$ MeV and $t_{1/2}=1800$ ms [13]. A γ-γ matrix gated on mass$=155$ and the 5.202-MeV α decay associated with the isomer was used to construct the level scheme of ^{155}Yb; the total projection is displayed in Fig. 4(a). The level structure of ^{155}Yb has been studied for the first time in the present experiment and is displayed in Fig. 5. The summary of the transitions is listed in Table II; the relative intensities were obtained from the total projection. The intensities of the transitions in the total projection and the systematics of the low-lying structures above the $7/2^{-}$ isomer in the $N=85$, even-Z isotones suggest that the 169.30-keV line is the $9/2^{-}\rightarrow7/2^{-}$ transition which populates the isomer. The spectrum gated on this transition is shown in Fig. 4(b).

The transitions at 223.4, 366.7, 474.7, and 755.1 keV cannot be placed. Although it is likely that the 169.30- and 815.7-keV transitions are in coincidence with the 223.4-, 366.7-, and 755.1-keV transitions, the statistics are insufficient to confirm the placements of these transitions in the level scheme.

C. Level scheme of ^{156}Lu

Two α-decaying isomers have been established in ^{156}Lu: a low-spin isomer with $E_\alpha=5.454$ MeV and $t_{1/2}=494$ ms and a high-spin isomer with $E_\alpha=5.565$ MeV and $t_{1/2}=198$ ms [13]. A γ-γ coincidence matrix gated on the high-spin isomeric α decay was constructed to establish the level scheme of ^{156}Lu; the total projection is displayed in Fig. 6(a). The coincidence spectrum gated on the strongest transition at 744.97 keV is shown in Fig. 6(b). The 744.97-keV transition is in coincidence with all of the other transitions associated with the isomer, except for the 364.89-keV transition.

The level scheme up to $I\gtrsim22^{+}$ and $E_x\sim5.3$ MeV above the high-spin isomer in ^{156}Lu, presented in Fig. 7, was con-

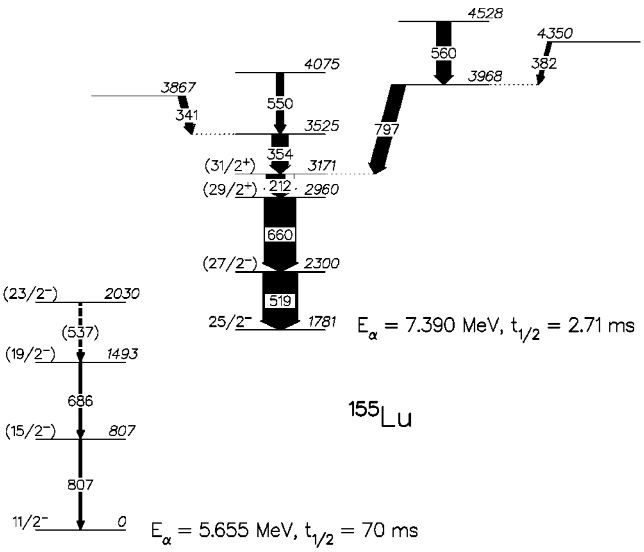

FIG. 3. Level structure above the $11/2^-$ and $25/2^-$ isomers in ^{155}Lu. The three transitions above the $11/2^-$ state are taken from Ref. [8] and assignments above the $25/2^-$ isomer are from the present measurement. The widths of the arrows are proportional to the γ-ray intensities.

structed primarily from coincidence relationships and intensity arguments from the γ-γ matrix associated with the $E_\alpha = 5.565$-MeV isomer. The excited states correlated with the decay of the high-spin isomer in ^{156}Lu are studied for the first time in the present measurement. The summary of the transitions assigned to ^{156}Lu is presented in Table III; the relative intensities of the transitions were obtained from the total projection of the matrix gated on mass=156 and $E_\alpha = 5.565$ MeV. A γ-γ coincidence matrix gated on mass 156, without an α-decay tag, was used to supplement the construction of the level scheme. The order of the 500.83-, 731.41-, and 1053.39-keV transitions is uncertain because these transitions have the same intensities within the statistical errors. The assignments of the spins and parities are based on the systematics of the excited states in the $N=85$ isotones [16–20], the angular distributions of the transitions, and intensity balance considerations. The assignment of a 10^+ $(\pi h_{11/2} \nu h_{9/2})$ state to the bottom of the cascade, instead of a 9^+ state, is based on the systematics of the excited states in the $N=85$ isotones, as discussed below.

The 364.89-keV transition in Fig. 6(a) is in coincidence with transitions at 304, 313, 524, 584, 761, and 776 keV, none of which are in coincidence with the 744.97-keV transition. These transitions may originate from the non-yrast states built upon the 9^+ isomer. The intensities of the strongest of these transitions in the total projection of the γ-ray events gated on the isomer associated with the 5.454-MeV α line in ^{156}Lu are also given in Table III. Because they are very weak, these transitions could not be placed in the level scheme.

The total projection [12] of the γ-ray events gated on the isomer associated with the 5.454-MeV α line in ^{156}Lu is contaminated by the tail of the more intense alpha line associated with the high-spin isomer. However, by subtracting the spectrum gated on the alpha decay of the high-spin isomer, a 162.21-keV transition can be assigned above the low-spin isomer in ^{156}Lu. Gamma-ray spectra were obtained by gating on the 162.21-keV transition in the γ-γ matrix gated on mass =156 alone, and in the matrix gated on mass =156 correlated with the $E_\alpha = 5.454$ MeV, but no coincidence relations could be established.

D. Level scheme of ^{157}Lu

One α decaying isomer has been identified [13] in ^{157}Lu, with $E_\alpha = 4.997$ MeV, $t_{1/2} = 4900$ ms, and it was assigned spin and parity $11/2^-$. Figure 8(a) displays the total projection of the γ-ray events gated on mass=157 and the α decays from both the isomer in ^{157}Lu and decay from the daughter, ^{153}Tm. This double correlation was imposed in order to minimize random contributions associated with the long time gate of ~15 s. The x rays from Lu isotopes are identified in this spectrum, which supports assignments of the transitions to ^{157}Lu. The total projections of the γ-ray

TABLE I. Energies, relative intensities, and placements of γ-ray transitions in ^{155}Lu above the $25/2^-$ isomer. Spins and parities in parentheses are based on systematics.

Energy (keV)	Intensity	Mult.	Excitation E_i (keV)	Excitation E_f (keV)	Assignment I_i^π	→	I_f^π
211.65(13)	572(114)	$(M1)$	3171	2960	$(31/2^+)$	→	$(29/2^+)$
341.3(3)	200(52)		3867	3525			
354.2(2)	463(97)		3525	3171			
381.8(4)	111(39)		4350	3968			
398.4(4)[a]	193(94)						
518.8(2)	≡1000	$(M1)$	2300	1781	$(27/2^-)$	→	$25/2^-$
549.6(4)	207(58)		4075	3525			
560.0(2)	432(96)		4528	3968			
659.7(2)	929(181)	$(E1)$	2960	2300	$(29/2^+)$	→	$(27/2^-)$
708.0(7)[a]	145(70)						
797.2(3)	392(95)		3968	3171			

[a]Not placed.

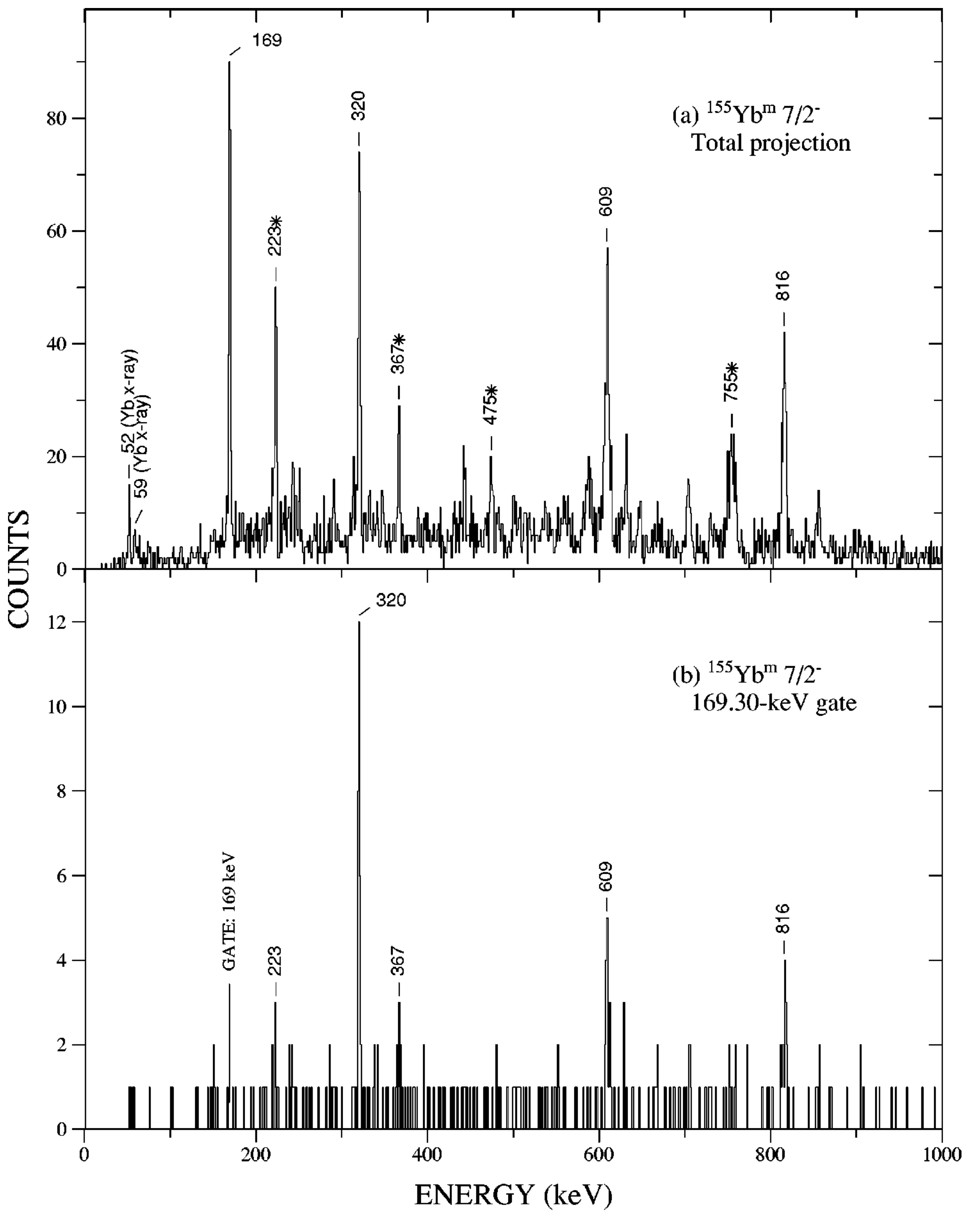

FIG. 4. (a) Total projection of γ-ray events gated on mass=155 and the α decays from the isomer in ^{155}Yb with $E_\alpha=5.202$ MeV and $t_{1/2}=1800$ ms. (b) Background-subtracted coincidence spectra gated on the 169.30-keV transition in ^{155}Yb.

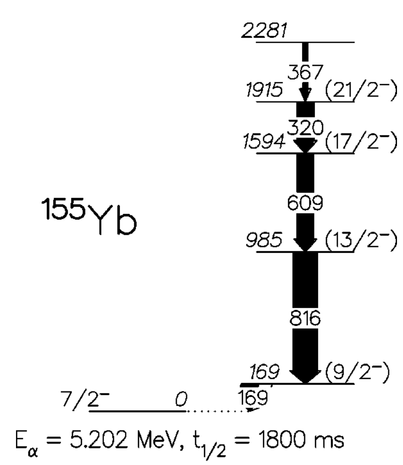

FIG. 5. Level structure above the 7/2$^-$ isomer in ^{155}Yb.

events gated on mass=157 and the α decay from ^{157}Lu, without requiring the ^{153}Tm daughter decay, and only on mass=157, which has enhanced statistics, are presented in Ref. [12] and are similar to the projection displayed in Fig. 8(a).

Three γ-γ coincidence matrices were constructed, gated on (1) mass=157, and the two sequential isomeric α decays in ^{157}Lu and in the daughter ^{153}Tm, (2) mass=157 and the isomeric α decay in ^{157}Lu, and (3) mass=157; the projections are displayed in Ref. [12]. Coincidence spectra gated on the 537.19-keV transition, the strongest transition in the total projections of these matrices, were found to be similar. Therefore the γ-γ matrix gated on mass=157 was used to construct the level scheme; the coincidence spectrum gated on the 537.19-keV transition from this matrix is presented in Fig. 8(b).

The extensive level scheme of ^{157}Lu above the 11/2$^-$ isomer, shown in Fig. 9, was constructed up to E_x

TABLE II. Energies, realtive intensities, and placements of γ-ray transitions in ^{155}Yb above the $7/2^-$ isomer. Spins and parities in parentheses are tentatively established.

Energy (keV)	Intensity	Mult.	Excitation E_i (keV)	E_f (keV)	Assignment I_i^π	→	I_f^π
169.30(12)	698(112)	$(M1)$	169	0	$(9/2^-)$	→	$7/2^-$
223.4(2) [a]	282(94)						
320.31(13)	659(94)	$(E2)$	1915	1594	$(21/2^-)$	→	$(17/2^-)$
366.7(2) [a]	185(71)		2281	1915			
474.7(4) [a]	140(83)						
609.3(2)	667(76)	$(E2)$	1594	985	$(17/2^-)$	→	$(13/2^-)$
755.1(3) [a]	468(129)						
815.7(3)	≡1000	$(E2)$	985	169	$(13/2^-)$	→	$(9/2^-)$

[a]Not placed.

~8.5 MeV and $I \gtrsim 45/2\hbar$. The relevant information on the transitions in ^{157}Lu are summarized in Table IV; relative intensities of the transitions were obtained from the spectrum gated on mass=157 and $E_\alpha = 4.997$ MeV. A DCO matrix was used to determine the multipolarity of the strong transitions. The arguments for the spin and parity assignments of the excited states were supplemented by angular distribution analyses and intensity balance requirements.

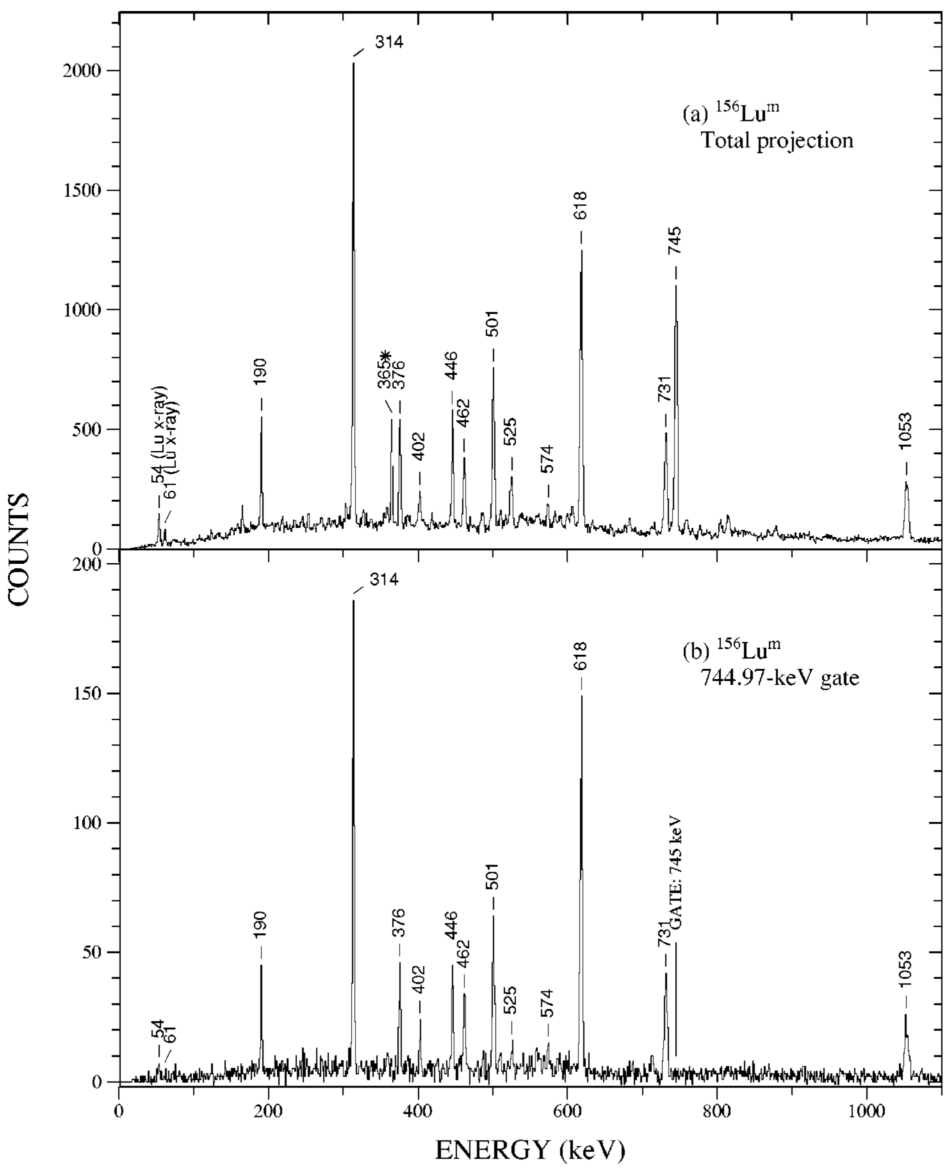

FIG. 6. (a) Total projection of γ-ray events gated on mass=156 and the α decay from the high-spin isomer in ^{156}Lu with $E_\alpha = 5.565$ MeV and $t_{1/2} = 198$ ms. The transition marked with an asterisk has not been placed in the level scheme. (b) Background-subtracted coincidence spectrum gated on the 744.97-keV transition in the matrix associated with the ^{156}Lu $E_\alpha = 5.565$ MeV isomeric decay.

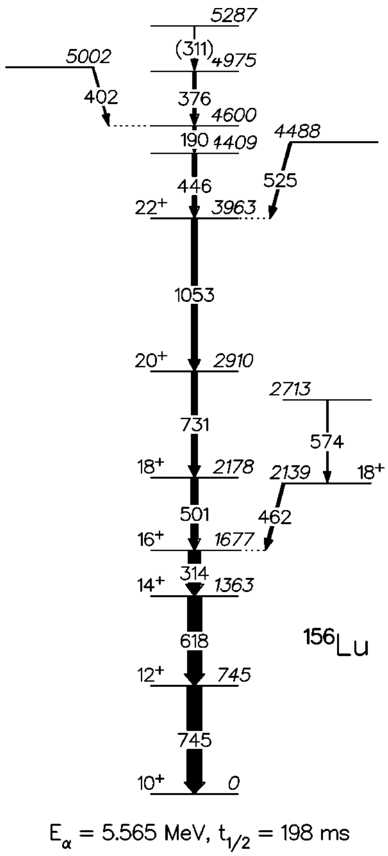

FIG. 7. Level structure above the high-spin isomer in ^{156}Lu. The 10^+ spin-parity assignment to the level at the bottom of the cascade is discussed in the text.

Four $E2$ cascades in ^{157}Lu are built above the low-lying states, two of positive and two of negative parity. The cascades with the same parity are connected by intraband $M1$, as well as crossover $E2$, transitions. Coincidence spectra gated on the 669.11- ($39/2^+ \rightarrow 35/2^+$), 469.35- ($37/2^+ \rightarrow 35/2^+$), and 199.73-keV ($39/2^+ \rightarrow 37/2^+$) transitions are presented in Ref. [12]. Although the 469.35- and 199.73-keV transitions are in coincidence with each other, the 669.11-keV transition is not in coincidence with either. Angular distributions suggest that the 669.11-keV transition is likely a stretched quadrupole and the 469.35- and 199.73-keV transitions are likely stretched dipole in character. Intensity balance arguments support the $M1$ assignments to both the 469.35- and 199.73-keV transitions. Similar arguments apply to the assignments of other $M1$ transitions, for which the placements are determined by the presence of crossover $E2$ transitions. At higher excitation energies, the level scheme is irregular and the intensities of the transitions are too low to allow multipolarity assignments.

IV. DISCUSSION

A. The $N=84$ isotone: ^{155}Lu

The systematics of the excitations above the $11/2^-$ isomers in the odd-Z, $N=84$ isotones are presented in Fig. 10. The sequences of states, $23/2^- \rightarrow 19/2^- \rightarrow 15/2^- \rightarrow 11/2^-$, are similar in excitation energies from ^{149}Tb to ^{155}Lu, which suggests that the same active particles are involved. These sequences in the odd-Z, $N=84$ isotones closely resemble the $6^+ \rightarrow 4^+ \rightarrow 2^+ \rightarrow 0^+$ sequences in the even-Z, $N=84$ isotones. The sequence in ^{155}Lu was first observed in Ref. [8], and suggested to be generated by coupling the unpaired $h_{11/2}$ proton to two $f_{7/2}$ neutrons.

TABLE III. Energies, relative intensities, a_2 angular distribution coefficients, and placements of γ-ray transitions in ^{156}Lu above the high-spin isomer.

Energy (keV)	Intensity	a_2	Mult.	E_x(keV) E_i	E_f	Assignment I_i^π	$\rightarrow$	I_f^π
190.48(10)	138(11)	−0.62(18)	$M1$	4600	4409			
304.3(3)[a]	24(6)							
311.2(4)	46(15)			5287	4975			
313.85(10)	773(33)	0.17(4)	$E2$	1677	1363	16^+	$\rightarrow$	14^+
364.89(11)[a]	102(7)							
375.81(10)	211(14)	0.18(4)	$E2$	4975	4600			
402.16(12)	81(10)			5002	4600			
446.29(10)	273(17)			4409	3963			
461.97(12)	168(12)	0.21(14)	$E2$	2139	1677	18^+	$\rightarrow$	16^+
500.83(10)	427(23)	0.37(7)	$E2$	2178	1677	18^+	$\rightarrow$	16^+
523.9(8) [a]	41(30)							
525.17(12)	144(11)			4488	3963			
574.2(2)	65(8)			2713	2139			
584.1(3) [a]	54(11)							
618.45(10)	936(42)	0.18(6)	$E2$	1363	745	14^+	$\rightarrow$	12^+
731.41(11)	413(23)	0.12(4)	$E2$	2910	2178	20^+	$\rightarrow$	18^+
744.97(10)	≡1000	0.12(6)	$E2$	745	0	12^+	$\rightarrow$	10^+
1053.39(12)	416(27)	0.35(13)	$E2$	3963	2910	22^+	$\rightarrow$	20^+

[a]Not placed.

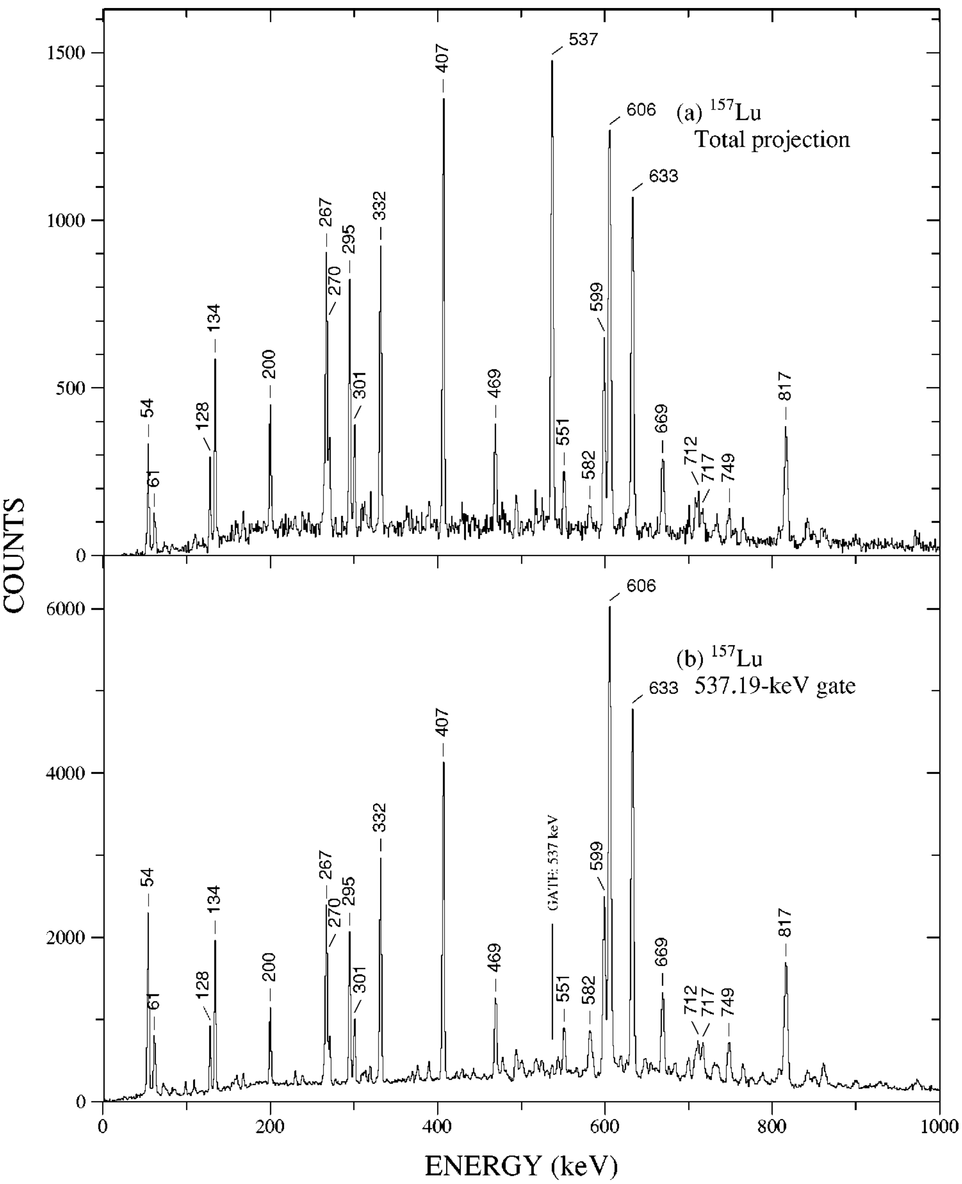

FIG. 8. (a) Total projection of γ-ray events gated on mass=157 and the α decay from the isomer in ^{157}Lu correlated with the α decay from the daughter, ^{153}Tm. (b) Background-subtracted coincidence spectrum gated on the 537.19-keV transition in the matrix gated on mass=157.

The yrast states in the $N=84$ isotones, from ^{149}Tb to ^{154}Yb [1,15,21,22] and in ^{156}Hf [8] have been assigned the $\pi h_{11/2}^{n} \nu f_{7/2}^{2}$ and $\pi h_{11/2}^{n} \nu f_{7/2} h_{9/2}$ configurations. The observed level energies of these multiparticle yrast states have been compared to shell model predictions, e.g., Ref. [1]. The strong attractive interaction between the protons in the $h_{11/2}$ orbital and the neutrons in the $h_{9/2}$ orbital was suggested to account for the inversion in Fig. 10 of the $25/2^-$ and the maximally aligned $27/2^-$ states in the $N=84$ isotones. The systematical lowering of the $\nu h_{9/2}$ single-particle states observed in the even-Z, $N=83$ isotones from ^{147}Gd to ^{153}Yb was the first evidence, e.g., Ref. [23], that the attractive interaction between $h_{11/2}$ protons and $h_{9/2}$ neutrons was changing the single-particle energies. This attractive interaction is expected to increase as the number of protons in the $h_{11/2}$ orbital increases. A corresponding decrease in the excitation energies of $\nu h_{9/2}$ states with respect to $\nu f_{7/2}$ excitations has been observed in the even-Z, $N=84$ isotones. For example, the $(\nu f_{7/2} h_{9/2})_{8^+}$ state is below the $(\nu f_{7/2})^2_{6^+}$ state in ^{156}Hf and results in the presence of an 8^+ isomer [8].

The $25/2^-$ states in Fig. 10 drop from an excitation energy of 2.628 MeV in ^{149}Tb to 1.781 MeV in ^{155}Lu, where this level is below the $23/2^-$ state. Therefore in ^{155}Lu the $25/2^-$ state can only decay via α emission [13], or electromagnetically by an $E4$ transition. The $25/2^-$ state has been suggested [22] to have the $\pi h_{11/2}^{3} \nu h_{9/2} f_{7/2}$ configuration, in which one of the $h_{11/2}$ protons is antialigned with the $h_{9/2}$ neutron to 1^+. The attractive proton-neutron interaction in this configuration lowers this state with respect to the $(\pi h_{11/2} \nu f_{7/2}^{2})_{23/2^-}$ state, causing the $25/2^-$ isomer. The transitions above the $25/2^-$ isomer in ^{155}Lu observed in the present measurement follow closely the systematics in the lighter, odd-Z isotones. The fully aligned $\pi h_{11/2} \nu f_{7/2} h_{9/2}$ configuration is suggested for the $27/2^-$ state, which is above the $25/2^-$ isomer. The $29/2^+$ and $31/2^+$ states are assigned the $\pi h_{11/2} \nu f_{7/2} i_{13/2}$ configuration from energy systematics.

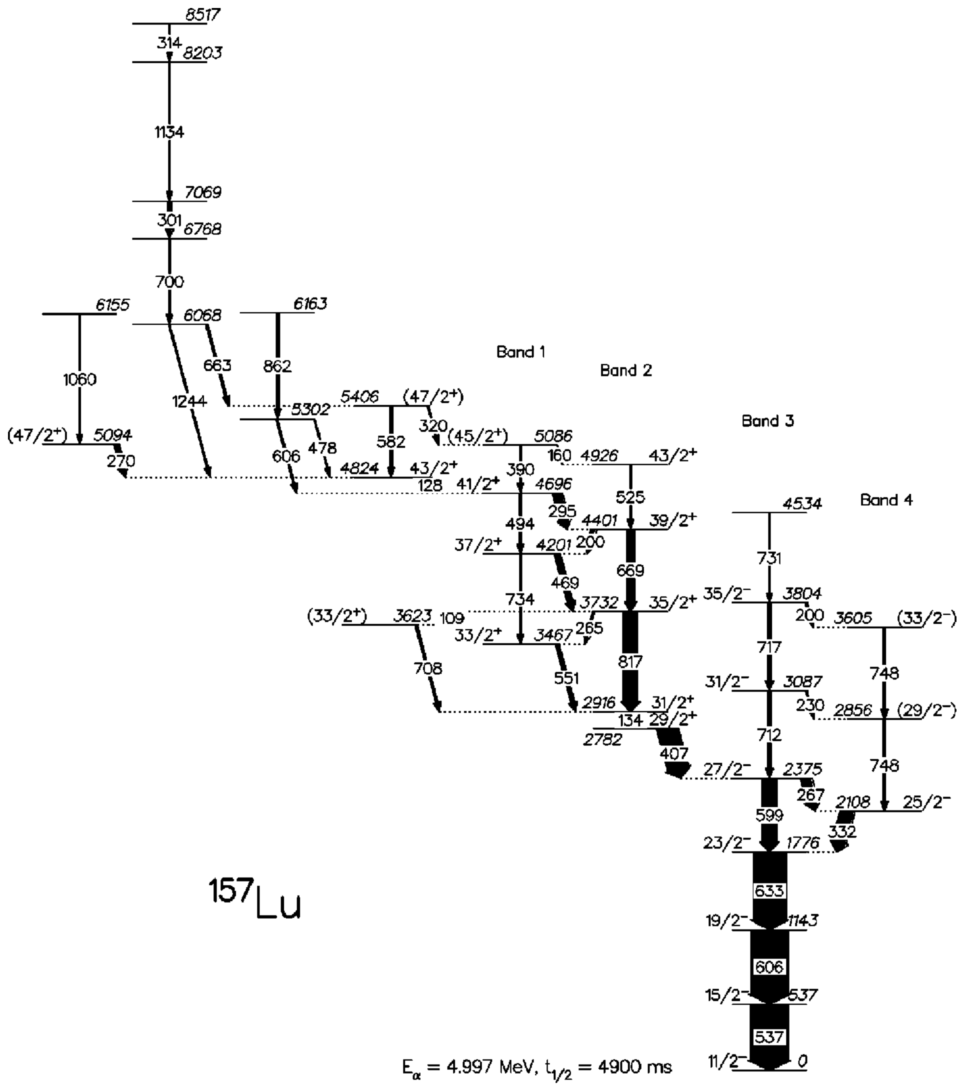

FIG. 9. Level structure above the $11/2^-$ isomer in ^{157}Lu.

B. The $N=85$ isotones: ^{155}Yb and ^{156}Lu

The $N=85$ isotones above ^{146}Gd have three valence neutrons outside of the $N=82$ closed shell, and valence protons outside of the $Z=64$ closed subshell. The Fermi surface of these nuclei is located near the $\pi h_{11/2}$ and $\nu f_{7/2}$ or $\nu h_{9/2}$ orbitals, which are close in energy. For the even-Z, $N=85$ isotones, the first few high-spin yrast states above the $7/2^-$ isomer can be generated by coupling the unpaired neutron in the $f_{7/2}$ or $h_{9/2}$ orbitals to the $(f_{7/2})^2$ states of the neutron core. As the number of protons increases, the energy difference between the $7/2^-$ and $9/2^-$ states decreases, because of the increase in the attractive proton-neutron interaction. For the odd-Z, $N=85$ isotones, a 9^+ isomer can result from the coupling between the unpaired $h_{11/2}$ proton and $f_{7/2}$ neutron. A low-lying 10^+ state can also be obtained from the coupling between $\pi h_{11/2}$ and $\nu h_{9/2}$.

The systematics of the cascades built upon the 10^+ states in the odd-Z isotones and the corresponding cascades built upon the $9/2^-$ states in the even-Z isotones are displayed in Fig. 11. The excitation energies of the $(\nu f^3_{7/2})_{7/2^-}$ states relative to the $(\nu f^2_{7/2} h_{9/2})_{9/2^-}$ states in the even-Z, $N=85$ isotones and of the 9^+ states relative to the 10^+ states in the odd-Z, $N=85$ isotones are also presented. In the even-Z, $N=85$ isotones, the energy spacings between the $7/2^-$ and $9/2^-$ states decrease dramatically as the number of protons increases. The cascade observed in the present work in ^{155}Yb follows the energy systematics of the excitations above the $7/2^-$ isomers in the even-Z, $N=85$ isotones. The energy spacing between the $7/2^-$ and $9/2^-$ states in the $Z=70$, ^{155}Yb is smaller than that in the $Z=68$ isotone, ^{153}Er [20], but larger when compared to that of the $Z=72$ isotone, ^{157}Hf [24]. Although the cascade built upon the $(\nu f^3_{7/2})_{7/2^-}$ state is yrast in ^{149}Gd, the $(\nu f^2_{7/2} h_{9/2})_{9/2^-}$ levels become yrast for $Z>64$. That no excitations built upon the $7/2^-$ isomers in ^{155}Yb and ^{157}Hf [24] were observed indicates that these excitations are above the yrast line.

A 10^+ state has been assigned to the bottom of the prompt cascade in ^{156}Lu observed in this experiment and displayed in Fig. 7. This assignment is supported by the systematical behavior of the cascades built above the $(\pi h_{11/2} \nu f^2_{7/2} h_{9/2})_{10^+}$

TABLE IV. Energies, relative intensities, DCO ratios, a_2 angular distribution coefficients, and placements of γ-ray transitions in ^{157}Lu above the $11/2^-$ isomer.

Energy (keV)	Intensity	R_{DCO}	a_2	Mult.	E_x(keV) E_i	E_f	Assignment I_i^π	$\rightarrow$	I_f^π
109.0(2)	22(4)			$M1$	3732	3623	$35/2^+$	$\rightarrow$	$(33/2^+)$
128.07(11)	80(6)	0.62(22)		$M1$	4824	4696	$43/2^+$	$\rightarrow$	$41/2^+$
133.90(10)	197(11)	0.51(12)		$M1$	2916	2782	$31/2^+$	$\rightarrow$	$29/2^+$
160.3(3)	13(3)			$(M1)$	5086	4926	$(45/2^+)$	$\rightarrow$	$43/2^+$
199.63(11)	<42			$(M1)$	3804	3605	$35/2^-$	$\rightarrow$	$(33/2^-)$
199.73(11)	111(8)	0.54(12)		$M1$	4401	4201	$39/2^+$	$\rightarrow$	$37/2^+$
230.1(3)	19(3)			$(M1)$	3087	2856	$31/2^-$	$\rightarrow$	$(29/2^-)$
265.4(3)	49(13)			$M1$	3732	3467	$35/2^+$	$\rightarrow$	$33/2^+$
267.23(12)	263(17)	0.65(16)	$-0.23(5)$	$M1$	2375	2108	$27/2^-$	$\rightarrow$	$25/2^-$
270.42(11)	125(7)	0.89(34)		$(E2)$	5094	4824	$(47/2^+)$	$\rightarrow$	$43/2^+$
294.92(10)	232(10)	0.76(20)	$-0.27(5)$	$M1$	4696	4401	$41/2^+$	$\rightarrow$	$39/2^+$
300.63(11)	91(6)	1.15(43)	0.25(5)	$E2$	7069	6768			
313.7(2)	<23				8517	8203			
319.6(2)	25(3)		$-0.39(26)$	$(M1)$	5406	5086	$(47/2^+)$	$\rightarrow$	$(45/2^+)$
331.83(10)	352(14)	0.59(14)	$-0.20(5)$	$M1$	2108	1776	$25/2^-$	$\rightarrow$	$23/2^-$
389.94(11)	<15			$(E2)$	5086	4696	$(45/2^+)$	$\rightarrow$	$41/2^+$
406.70(10)	575(22)	0.55(6)	$-0.35(2)$	$E1$	2782	2375	$29/2^+$	$\rightarrow$	$27/2^-$
469.35(11)	163(9)	0.86(19)	$-0.16(5)$	$M1$	4201	3732	$37/2^+$	$\rightarrow$	$35/2^+$
477.8(2)	29(4)				5302	4824			
494.5(2)	48(6)		0.46(10)	$E2$	4696	4201	$41/2^+$	$\rightarrow$	$37/2^+$
524.9(3)	37(5)		1.59(35)	$E2$	4926	4401	$43/2^+$	$\rightarrow$	$39/2^+$
537.19(10)	$\equiv 1000$		0.11(3)	$E2$	537	0	$15/2^-$	$\rightarrow$	$11/2^-$
551.16(14)	96(7)		$-0.43(15)$	$M1$	3467	2916	$33/2^+$	$\rightarrow$	$31/2^+$
582.1(2)	55(6)			$(E2)$	5796	5214	$(47/2^+)$	$\rightarrow$	$(43/2^+)$
599.27(11)	375(16)	1.03(15)		$E2$	2375	1776	$27/2^-$	$\rightarrow$	$23/2^-$
605.0(5)	<92				6768	6163			
605.8(5)	<92				5302	4696			
605.83(10)	977(32)	1.14(16)		$E2$	1143	537	$19/2^-$	$\rightarrow$	$15/2^-$
632.80(12)	882(39)	1.19(18)		$E2$	1776	1143	$23/2^-$	$\rightarrow$	$19/2^-$
662.9(3)	<56				6068	5406			
669.11(12)	202(12)	1.02(18)	0.28(6)	$E2$	4401	3732	$39/2^+$	$\rightarrow$	$35/2^+$
700.1(3)	44(6)				6768	6068			
708.0(2)	57(8)		$-0.38(10)$	$(M1)$	3623	2916	$33/2^+$	$\rightarrow$	$31/2^+$
711.7(4)	78(8)		0.33(10)	$E2$	3087	2375	$31/2^-$	$\rightarrow$	$27/2^-$
717.0(2)	86(8)		0.39(6)	$E2$	3804	3087	$35/2^-$	$\rightarrow$	$31/2^-$
730.5(5)	41(5)				4534	3804			
734.4(4)	38(5)		0.44(12)	$E2$	4201	3467	$37/2^+$	$\rightarrow$	$33/2^+$
748.4(5)				$(E2)$	3605	2856	$(33/2^-)$	$\rightarrow$	$(29/2^-)$
748.5(5)	}106(9)			$(E2)$	2856	2108	$(29/2^-)$	$\rightarrow$	$25/2^-$
816.52(12)	375(19)	0.96(17)	0.23(4)	$E2$	3732	2916	$35/2^+$	$\rightarrow$	$31/2^+$
861.7(3)	55(6)				6163	5302			
1060.3(4)	41(7)				6155	5094			
1134.5(5)	25(6)				8203	7069			
1244.0(4)	38(7)				6068	4824			

and the $(\pi h_{11/2} \nu f^3_{7/2})_{9^+}$ configurations in the odd-Z, $N=85$ isotones. In addition, the cascade observed in ^{156}Lu is similar to the one built upon the $9/2^-$ state in ^{155}Yb. Just as the energy differences between $(\nu f^3_{7/2})_{7/2^-}$ and $(\nu f^2_{7/2} h_{9/2})_{9/2^-}$ excitations decrease in the even-Z, $N=85$ isotones, the energy differences between the corresponding 9^+ and 10^+ states in the odd-Z isotones are reduced by the increase in the attractive proton-neutron interaction as the number of valence protons increases.

From the present measurement, it is difficult to determine whether the 9^+ state is above or below the 10^+ state in ^{156}Lu. The energy systematics in Fig. 11 suggest that the 10^+

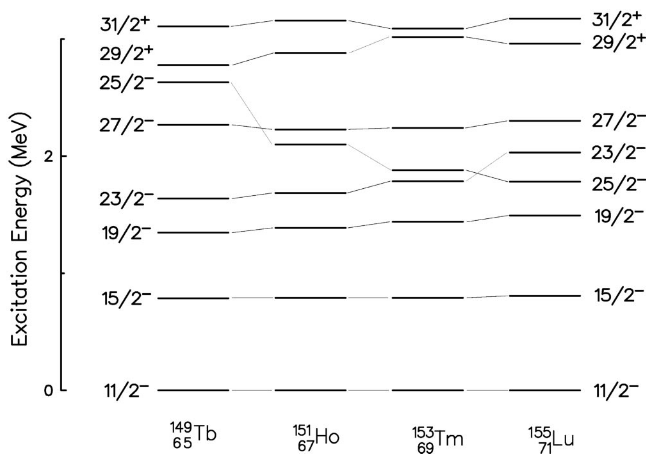

FIG. 10. Systematics of the low-lying yrast states above the $11/2^-$ isomers in the odd-Z, $N=84$ isotones, taken from Refs. [1,15,8] and the present work. Prompt excitations above the $25/2^-$ isomer in ^{155}Lu are from the present work.

state is probably located above the 9^+ state in ^{156}Lu and thus the high-spin isomer observed in ^{156}Lu is associated with the 9^+ state. However, these two states are probably very close in excitation energy. Therefore the 10^+ to 9^+ transition energy could be very small (<100 keV) and the associated $M1$ transition would have a large conversion coefficient ($\alpha_{\mathrm{tot}} \geqslant 3.82$).

The excitations in the light odd-Z, $N=85$ isotones in Fig. 11 suggest that the excitation energy of the 11^+ state built on the $(\pi h_{11/2} \nu f^3_{7/2})_{9^+}$ configuration could be comparable to that of the 12^+ state in the cascade built upon the 10^+ state. As a result, the cascade built upon the $(\pi h_{11/2} \nu f^3_{7/2})_{9^+}$ configuration would be non-yrast and hence could be populated too weakly in the present measurement to be observed. The unassigned transitions in Table III, associated with the high-spin isomeric decay, are probably associated with the de-excitation of the states built upon the 9^+ isomer.

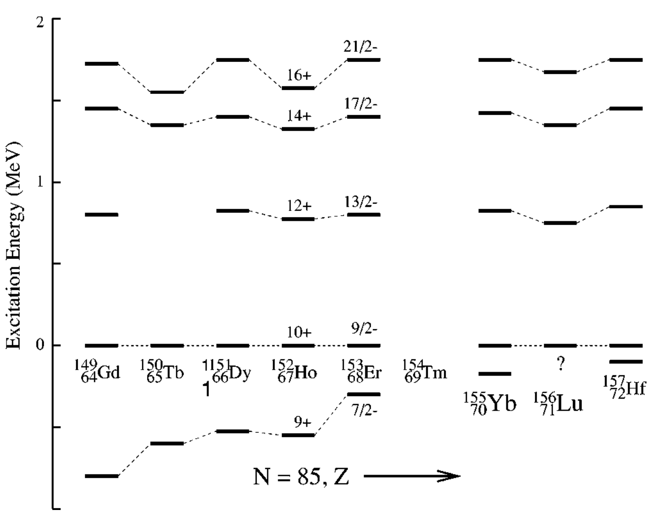

FIG. 11. Systematics of the cascades built on the $(\pi h_{11/2} \nu f^2_{7/2} h_{9/2})_{10^+}$ states in the $N=85$ isotones, taken from Refs. [16–20] and the present work. The excitation energies of the $(\nu f^3_{7/2})_{7/2^-}$ states relative to the $(\nu f^2_{7/2} h_{9/2})_{9/2^-}$ states in the even-Z, $N=85$ isotones are also displayed.

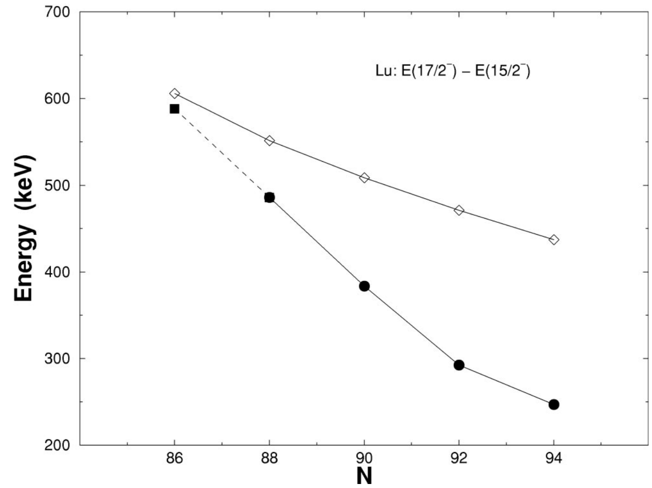

FIG. 12. Systematics of the energies of the $17/2^- \to 15/2^-$ (solid symbols) and $19/2^- \to 15/2^-$ (open symbols) transitions in Lu isotopes, taken from Refs. [25–27] and the present work. The energy of the $17/2^- \to 15/2^-$ transition is linearly extrapolated to ^{157}Lu.

C. Level structure of ^{157}Lu

The low-lying states of ^{157}Lu have very similar energy spacings, which suggests that ^{157}Lu is a transitional nucleus with a low-lying vibrational structure. The signature $\alpha = +1/2$ decay sequence observed in the heavier isotopes is not observed in ^{157}Lu. The systematics of the energy splittings between the signature partner bands, the $17/2^- \to 15/2^-$ transition energy, in the $h_{11/2}$ sequences for the heavier odd-Lu isotopes is shown in Fig. 12. Extrapolation of this transition energy to ^{157}Lu suggests that the energy of the $17/2^- \to 15/2^-$ transition is close to that of the $19/2^- \to 15/2^-$ transition, as expected, since these states would be degenerate if ^{157}Lu is spherical. As a result, the $\alpha = +1/2$ decay sequence in ^{157}Lu is above the yrast line and would be weakly populated and therefore difficult to observe.

The $E2$ cascades above the vibrational structure observed in ^{157}Lu are similar to the signature partner bands at high spin observed in the heavier Lu isotopes. Because the ^{157}Lu cascades do not extend to many transitions, extensive study of $B(M1)/B(E2)$ ratios similar to those done on the heavier Lu isotopes, e.g., Ref. [25], is not available. The $B(M1)/B(E2)$ ratios for the levels in bands 1, 2, and 3 in ^{157}Lu and the corresponding levels in ^{161}Lu are compared in Table V. The $B(M1)/B(E2)$ ratios in ^{157}Lu are consistently larger than those in ^{161}Lu. Such results are expected because ^{157}Lu is a transitional nucleus, which is only slightly deformed, and therefore has smaller $B(E2)$ values compared to those in the heavier isotopes.

V. SUMMARY

The ^{102}Pb(^{58}Ni, $xnyp$) reaction at $E_{\mathrm{beam}} = 270$ MeV was used to study proton-rich $N=84,85$ isotones and ^{157}Lu. Excited states up to $E_x \sim 4.5$ MeV and $I \gtrsim 31/2\hbar$ above the

TABLE V. $B(M1)/B(E2)$ values for the three $E2$ bands observed in ^{157}Lu compared to the corresponding values in ^{161}Lu [25].

Band	Spin (I^π)	$\frac{B(M1:I\to I-1)}{B(E2:I\to I-2)}$	
		^{157}Lu	^{161}Lu
1	$37/2^+$	17(5)	0.9(1)
	$41/2^+$	6(2)	0.9(2)
2	$35/2^+$	1.2(2)	1.16(10)
	$39/2^+$	7.9(4)	1.15(10)
3	$27/2^-$	2.3(1)	<0.31
	$31/2^-$	1.8(2)	2.7(3)

$25/2^-$ isomer in ^{155}Lu, $E_x\sim 2.3$ MeV and $I\gtrsim 21/2\hbar$ above the $7/2^-$ isomer in ^{155}Yb, $E_x\sim 5.3$ MeV and $I\gtrsim 22\hbar$ above the high-spin isomer in ^{156}Lu, and $E_x\sim 8.5$ MeV and $I \gtrsim 45/2\hbar$ in ^{157}Lu have been identified.

The energy levels in ^{155}Lu above the $11/2^-$ isomer follow the energy systematics displayed by the odd-Z, $N=84$ isotones up to spin $= 31/2^+$. The systematical lowering of the $25/2^-$ states is understood by the increase in the strong attractive interaction between the $h_{11/2}$ proton and $h_{9/2}$ neutron with the increase in proton number.

In ^{155}Yb, the energy difference between the $7/2^-$ and $9/2^-$ states follows the systematics of other even-Z, $N=85$ isotones. The systematical lowering of the $9/2^-$ state with respect to the $7/2^-$ state is again explained by the increase in the strong attractive interaction between the protons in the $h_{11/2}$ orbital and the neutrons in the $h_{9/2}$ orbital. The excitations above the $9/2^-$ state can be generated by the coupling of the unpaired $h_{9/2}$ neutron to the neutron $(f^2_{7/2})$ excitations in the core.

In ^{156}Lu, the energy systematics of the $N=85$ isotones was invoked to deduce a 10^+ assignment for the level at the bottom of the prompt cascade correlated with the α decay of the high-spin isomer. In particular, the energy spacings of the first four levels in ^{156}Lu are very similar to those of levels built upon the $9/2^-$ state in ^{155}Yb. The preferential population of yrast states built on the $(\pi h_{11/2}\nu h_{9/2})_{10^+}$ configuration over non-yrast levels built on $(\pi h_{11/2}\nu f_{7/2})_{9^+}$ has been suggested to explain why excitations built on the 9^+ configuration have not been identified. Although the energy systematics of the $N=85$ isotones suggest that the attractive interaction between the $h_{11/2}$ protons and $h_{9/2}$ neutrons in ^{156}Lu is not sufficiently strong to lower the 10^+ state to below the 9^+ level, these two states are probably very close in energy.

From the energy systematics of the Lu isotopes, and the approximately equal energy spacings at low excitations, a vibrational structure is proposed above the $11/2^-$ isomer in ^{157}Lu. At higher excitations, two positive-parity and two negative-parity $E2$ cascades, with $M1$ intraband transitions, have been identified. Although these cascades are not as extensive as those observed in the heavier Lu isotopes, e.g., Ref. [25], $B(M1)/B(E2)$ ratios in ^{157}Lu are consistent with a less deformed structure, compared to that of heavier Lu isotopes.

It is possible that new phenomena could be observed in nuclei, such as ^{155}Lu, which are near the proton-drip line and in which the last proton is only weakly bound. The present analysis, which focused on the systematical behavior of excitation energies as functions of proton and neutron numbers, indicated that the structure of ^{155}Lu is similar to that of its lighter isotones. To test more quantitatively the structure of nuclei near and beyond the proton-drip line, shell model calculations are needed to determine the extent to which single-particle spacings and interaction matrix elements, appropriate for more stable nuclei, remain valid at the limit of stability.

ACKNOWLEDGMENTS

This work was supported in part by U.S. National Science Foundation and the Department of Energy – Nuclear Physics Division under Contract Nos. W-31-109-ENG-38 and DE-AC03-76SF00098.

[1] C.T. Zhang *et al.*, Phys. Rev. C **54**, R1 (1996).
[2] P. Kleinheinz, S. Lunardi, M. Ogawa, and M.R. Maier, Z. Phys. A **284**, 315 (1978).
[3] M. Ogawa, R. Broda, K. Zell, P.J. Daly, and P. Kleinheinz, Phys. Rev. Lett. **41**, 289 (1978).
[4] P. Kleinheinz, R. Broda, P.J. Daly, S. Lunardi, M. Ogawa, and J. Blomqvist, Z. Phys. A **290**, 295 (1979).
[5] P. Kleinheinz *et al.*, Inst. Phys. Conf. Ser. **132**, 691 (1993).
[6] S. Hofmann *et al.*, Z. Phys. A **333**, 107 (1989).
[7] A. Kuhnert *et al.*, Phys. Rev. C **46**, 484 (1992).
[8] D. Seweryniak *et al.*, Proceedings of the Conference on Nuclear Structure at the Limits, Argonne, 1996, ANL/PHY-97/1, 1997, p. 247.
[9] K.Y. Ding *et al.*, Phys. Rev. C **62**, 034316 (2000).
[10] C.N. Davids *et al.*, Nucl. Instrum. Methods Phys. Res. B **70**, 358 (1992).
[11] E.S. Paul *et al.*, Phys. Rev. C **51**, 78 (1995).
[12] K.Y. Ding, Ph.D. dissertation, Rutgers University, 1999.
[13] R. Page, P.J. Woods, R.A. Cunningham, T. Davinson, N.J. Davis, A.N. James, K. Livingston, P.J. Sellin, and A.C. Shotter, Phys. Rev. C **53**, 660 (1996).
[14] K.S. Toth and W. Nazarewicz, Phys. Rev. C **48**, R978 (1993).
[15] Z. Méliani *et al.*, Nucl. Phys. **A575**, 221 (1994).
[16] M. Piiparinen *et al.*, Z. Phys. A **300**, 133 (1981).
[17] G. Duchêne *et al.*, Z. Phys. A **350**, 39 (1994).
[18] M. Piiparinen, S. Lunardi, P. Kleinheinz, H. Backe, and J. Blomqvist, Z. Phys. A **290**, 337 (1979).
[19] S. André, C. Foin, D. Santos, D. Barnéoud, J. Genevey, Ch. Vieu, J.S. Dionisio, M. Pautrat, C. Schück, and Z. Méliani, Nucl. Phys. **A575**, 155 (1994).
[20] C. Foin, S. André, D. Barnéoud, G. Bastin, A. Peghaire, and J.P. Thibaud, Z. Phys. A **305**, 81 (1982).

[21] M.A. Deleplanque, J.C. Bacelar, E.M. Beck, R.M. Diamond, F.S. Stephens, J.E. Draper, Th. Dossing, and K. Neergard, Phys. Lett. B **195**, 17 (1987).
[22] C.T. Zhang, P. Kleinheinz, M. Piiparinen, R. Collatz, T. Lönnroth, G. Sletten, and J. Blomqvist, Z. Phys. A **348**, 249 (1994).
[23] J.H. McNeill, A.A. Chishti, P.J. Daly, W. Gelletly, M.A.C. Hotchkis, M. Piiparinen, B.J. Varley, P.J. Woods, and J. Blomqvist, Z. Phys. A **344**, 369 (1993).
[24] A.F. Saad *et al.*, Z. Phys. A **351**, 247 (1995).
[25] C.-H. Yu *et al.*, Nucl. Phys. **A489**, 477 (1988).
[26] Y. Ma, H. Sun, Y. Liu, S. Wen, H. Zheng, S. Li, G. Li, G. Yuan, P. Weng, and C. Yang, J. Phys. G **21**, 937 (1995).
[27] *Table of Isotopes*, edited by R.B. Firestone, V.S. Shirley, C.M. Baglin, S.Y.F. Chu, and J. Zipkin, 8th ed. (Wiley, New York, 1996).